Collision of a suddenly released bent carbon nanotube with a circular graphene sheet

W. H. Duan' , C. M. Wang, and W. X. Tang

Citation: Journal of Applied Physics **107**, 074303 (2010); doi: 10.1063/1.3330754
View online: http://dx.doi.org/10.1063/1.3330754
View Table of Contents: http://aip.scitation.org/toc/jap/107/7
Published by the American Institute of Physics

Collision of a suddenly released bent carbon nanotube with a circular graphene sheet

W. H. Duan,[1,a)] C. M. Wang,[2] and W. X. Tang[3]
[1]*Department of Civil Engineering, Monash University, Clayton, Victoria 3800, Australia*
[2]*Engineering Science Programme, Faculty of Engineering, National University of Singapore, Kent Ridge, Singapore 119260, Singapore*
[3]*Department of Physics, Monash University, Clayton, Victoria 3800, Australia*

(Received 21 December 2009; accepted 30 January 2010; published online 5 April 2010)

Molecular dynamics (MD) simulations were used to investigate the mechanical strain energy release of a bent single wall carbon nanotube (CNT) and its mechanical collision with a circular graphene sheet that is fixed at its edges. The MD simulations show that the CNT is able to store a vast amount of mechanical strain energy because of the formation of kinks on its wall at the regions of maximum curvature. The sudden release of the strain energy upon releasing the bent CNT can cause its tip to approach a speed of 7000 m/s. Even with such a high speed collision with a monolayer graphene sheet, the CNT and the monolayer graphene sheet remain completely intact and do not suffer any damage. The instantaneous average impact pressure between the CNT and the graphene sheet is calculated to be in the range of 1–10 GPa for different temperatures and aspect ratios of the CNT. These results indicate the promising application of a CNT and a graphene sheet as a nanoknife and a nanocutting board, respectively, for nanocleavage processes such as sequence-specific DNA cleaving processes. © *2010 American Institute of Physics*. [doi:10.1063/1.3330754]

I. INTRODUCTION

Carbon nanotubes (CNTs) and graphene sheets have been intensively studied by engineers and scientists due to their remarkable physical properties. CNTs are macromolecules of carbon in a periodic hexagonal arrangement with a cylindrical shell shape.[1] They are highly flexible and are able to withstand significant compression, elongation, twisting, and bending in a reversible manner and without suffering fracture or plastic deformation.[2] CNT Young's modulus exceeds 1 TPa when the wall thickness is assumed to be 0.34 nm (Ref. 3) and its tensile strength is in the tens of gigapascal.[4] Moreover, its elastic strain has been demonstrated experimentally to reach up to 6%,[5] while molecular dynamics (MD) models predict reversible tensile strains as high as 20%.[6–8] On the other hand, a single flat layer of carbon is dubbed a graphene sheet. Research studies have been undertaken to measure the effective spring constant of suspended graphene sheets by utilizing an atomic force microscope (AFM).[9] Its effective spring constant was found to be of the order of 1 to 5 N/m and its Young's modulus to be about 0.5 TPa, which differs from the bulk graphite Young's modulus of 1 TPa. Recently, Poot and van der Zant[10] used the AFM to measure the nanomechanical properties of graphene sheets that were suspended over circular holes. Booth *et al.*[11] reported a macroscopic size of graphene sheet and demonstrated graphene sheet having a very large stiffness to support extremely large loads; millions of times exceeding their own weight. Their findings revealed that graphene sheets can sustain very large bending and stretching prior to the occurrence of fracture.

The super mechanical properties make CNTs a promising candidate for application as an energy supplier in microelectromechanical and nanoelectromechanical systems. Král and Tománek[12] proposed a laser-driven pump for atomic transport through CNTs. A two beam coherent control is used to inject a carrier population into the lowest unoccupied nanotube bands, which is anisotropic in momentum space. The resulting electron current moves intercalated atoms along the tube. Chang[13] demonstrated that the van der Waals (vdW) potential energy stored in CNTs with diameters greater than 3.5 nm can be released by the domino process, allowing a CNT to be an energy provider. Molecules C60 inside a single-walled CNT can be accelerated by the domino wave and finally shot out at a speed of 1.13 km/s. Insepov *et al.*[14] and Wang[15,16] investigated the feasibility of pumping atoms through CNTs. Hill *et al.*[17] presented a concept of a portable electric power source that stores energy in a highly ordered arrays of CNTs. Motivated by these creative endeavors in using CNTs as energy suppliers, we explore the potential and feasibility of using a CNT as a mechanical *nanoknife* and a graphene sheet as a *nanocutting board*. For a CNT to function as a mechanical knife, we propose that the CNT be first bent elastically backward into a bow shape and then locked in this bent configuration in order to store the strain energy until used. This process can be realized by 3D nanomanipulation techniques such as nanomanipulators, nanogrippers,[18–20] and optical tweezers.[21] When the bent CNT is released suddenly, the stored energy is transmitted to the desired objects, which can be laid on a graphene sheet. The high impact pressure between the CNT and graphene sheet due to the impulsive collision can be utilized in nanocleavage processes such as sequence-specific protein cleaving process.[22,23]

[a)]Author to whom correspondence should be addressed. FAX: +61-3-99054944. Electronic mail: wenhui.duan@eng.monash.edu.au.

In this paper, we perform MD simulations on the strain energy release of a bent CNT and its collision process with a circular, monolayer graphene sheet that is fixed at its edges. The total potential energy is decomposed into internal bond energy and nonbonded energy and their roles in these processes are explored. The energy transfer between the potential energy and the kinetic energy, the deformation of the CNT and graphene sheet, and the impact pressure due to mechanical collision are investigated. The effectiveness of the CNT and graphene sheet acting as a knife and cutting board in terms of different aspect ratios of CNTs and temperature is also assessed.

II. ATOMISTIC MODELING USING COMPASS FORCE FIELD

MD simulations involve an initial geometry optimization (using the conjugate-gradient method) for the bent CNT while restraining the carbon atoms at the ends from moving. The resulting energy minimized CNT and graphene sheet will then be subjected to an NVT-ensemble (i.e., the canonical ensemble, the number of particles (N), the volume (V), of each system in the ensemble are the same, and the ensemble has a well defined temperature (T), given by the temperature of the heat bath with which it would be in equilibrium) MD simulation of 100 ps at a prescribed temperature during which the entire system reached thermodynamic equilibrium. This NVT stage will be followed by a NVE (i.e., the microcanonical ensemble, all copies of the system have the same number of particles (N), the same volume (V) and the same energy (E)) MD simulation of 100 ps. The present analysis will focus on this NVE stage, during which the top end of the bent CNT is released and allowing the CNT to collide with a circular graphene sheet. The data collection is performed at a time step of 10 fs for subsequent statistical analyses.

The atomic interaction is modeled by the condensed-phased optimized molecular potential for atomistic simulation studies (COMPASS) force field,[24] which is the first *ab initio* force field that was parameterized and validated using condensed-phase properties. This force field has been proven to be applicable in describing the mechanical properties of CNTs.[25,26] In the COMPASS force field, the total potential energy E is expressed as follows:[27]

$$E = \sum E^{(b)} + \sum E^{(\theta)} + \sum E^{(\phi)} + \sum E^{(\chi)} + \sum E^{(bb')} + \sum E^{(b\theta)} + \sum E^{(b\phi)} + \sum E^{(b'\phi)} + \sum E^{(\theta\theta')} + \sum E^{(\theta\phi)} + \sum E^{(\theta\theta'\phi)} + \sum E^{(\mathrm{vdw})} + \sum E^{(\mathrm{elec})}, \quad (1)$$

where b and b' are the lengths of two adjacent bonds, θ and θ' are the adjacent two-bond angles, ϕ is the dihedral torsion angle, and χ is the out-of-plane angle. The total potential energy may be divided into two categories, namely,

(1) contributions from each of the internal valence coordinates and their cross-coupling items, i.e., $\Sigma E^{(b)}$, $\Sigma E^{(\theta)}$, $\Sigma E^{(\phi)}$, $\Sigma E^{(\chi)}$, $\Sigma E^{(bb')}$, $\Sigma E^{(b\theta)}$, $\Sigma E^{(b\phi)}$, $\Sigma E^{(b'\phi)}$, $\Sigma E^{(\theta\theta')}$, $\Sigma E^{(\theta\phi)}$, and $\Sigma E^{(\theta\theta'\phi)}$, and
(2) nonbonded interactions, i.e., the vdW energy, $\Sigma E^{(\mathrm{vdw})}$, and the Coulomb electrostatic energy, $\Sigma E^{(\mathrm{elec})}$.

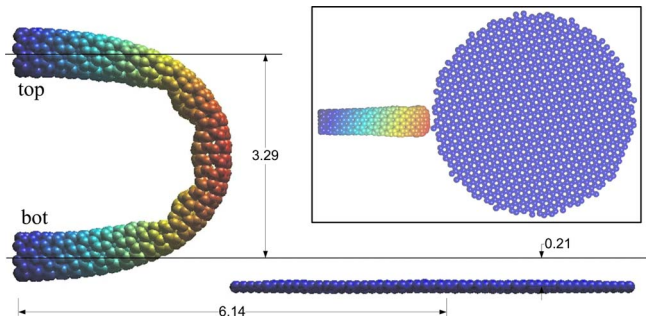

FIG. 1. (Color online) MD model for the first scenario, i.e., a zigzag (8, 0) CNT and a circular graphene sheet with a radius of 2.8 nm. The inset is the top view of the model. The length of the zigzag CNT is 8.52 nm and its diameter is 0.62 nm. The two ends of the CNT are denoted as "top" and "bot," respectively. The longitudinal axis of the CNT is 0.21 nm above the graphene sheet plane and aligned with the diameter of the graphene sheet. The horizontal distance between the bot end of the CNT and the center of the graphene sheet is set as 6.14 nm. The bending deformation was applied to the zigzag (8, 0) CNT. Carbon atoms with high strains concentrated at the kinks are highlighted. The distance between the two ends of the CNT is set at 3.29 nm. Two layers of carbon atoms of the circular graphene sheet at the boundary were constrained from moving so as to simulate a clamped edge condition.

The full expressions for these energy terms are given in Ref. 27.

III. RESULTS AND DISCUSSION

In order to investigate the collision of a CNT and a graphene sheet and their feasibility as a nanoknife and a nanocutting board, respectively, three scenarios of collisions are explored. The first scenario is the collision of a zigzag (8, 0) CNT with an aspect ratio of 13 and a circular graphene sheet with a radius of 2.8 nm subject to room temperature 300 K as shown in Fig. 1. To investigate the effect of temperature and aspect ratio of CNTs on the impact pressure, two variations from the first scenario, i.e., 1500 K and a zigzag (8, 0) CNT with an aspect ratio of 10, are adopted for the second and third scenarios, respectively. In the third scenario, the longitudinal axis of the CNT is 0.21 nm above the graphene sheet plane and is aligned with the diameter of the graphene sheet. The horizontal distance between the top end of the CNT and the center of the graphene sheet is set at 5.16 nm. The bending deformation was applied to the CNT and the distance between the two ends of the CNT is set at 2.53 nm.

A. Energy in collision process

Figure 1 shows the MD model in the first scenario, i.e., a zigzag (8, 0) CNT with its top end bent backward and a circular graphene sheet placed at a prescribed distance from the CNT. The strain energy release starts when the top end of the bent CNT is unlock and it ends before the CNT touches the graphene sheet. During this stage, we have the alternate conversions of the potential and kinetic energies of the CNT. Interestingly, the release process of the potential energy of the CNT is not smooth because of the recovery phenomenon and the propagation of kinks. The potential energy snaps out at the following times: 3.5, 6.7, and 10 ps, as shown in Fig.

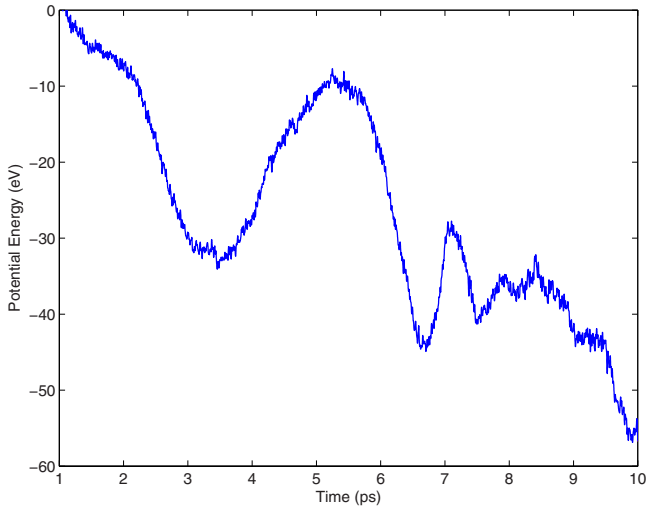

FIG. 2. (Color online) Variation in potential energy of the CNT in the first scenario (collision of CNT with aspect ratio of 13 and graphene sheet at room temperature). The strain energy snaps out three times, i.e., 3.5 ps, 6.8 ps, and 10 ps, respectively.

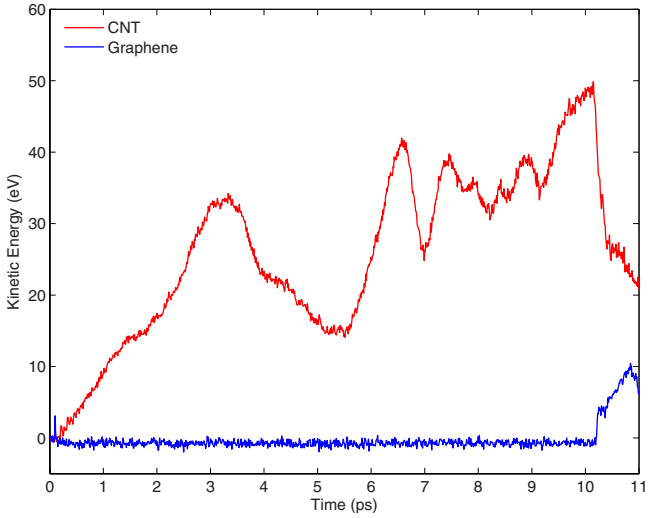

FIG. 4. (Color online) Variations of kinetic energies of CNT and graphene sheet during strain energy release process in the first scenario (collision of CNT with aspect ratio of 13 and graphene sheet at room temperature).

2. The corresponding snapshots of the CNT at these times are plotted in Figs. 3(a)–3(c). Note that there are four kinks located at the CNT wall and these kinks are spaced out in the mid portion of the CNT as shown in Fig. 1. The mid portion corresponds to the region with maximum bending curvature. When the top end of the bent CNT is suddenly released, three of these kinks disappeared while the remaining kink propagated to the bottom held end of CNT as shown in Figs. 3(a) and 3(b). In Fig. 3(c), the remaining kink on the left end propagated to the right end of CNT with a speed of approximately 240 m/s. The observations are in agreement with the result that was predicted by Wang.[15] One may deduce that the kinks in CNTs can be used to store the potential energy and its deformation is elastic and can be fully recovered. This is in line with the knowledge that kinks in CNT wall can be used as energy storage in nanodevices.[15,16,28]

The strain energy release stage is completed after about 10 ps. At this point, the potential energy of CNT is fully released resulting in the CNT having the maximum kinetic energy as shown in Fig. 4. The velocity of the atoms at the top end of the CNT increases to 4260 m/s while the graphene sheet remains at rest, thereby setting up a high speed collision condition. The value of the velocity is of the same order as the trinitrotoluene detonation velocity[29] of 6900 m/s, indicating that CNT can be used as a nanomechanical knife to cut materials.

The oscillations of vdW energy of the CNT and graphene sheet in a high speed collision process are plotted in Fig. 5(a). It can be clearly seen that there are five strong repeated collisions between the CNT and the graphene sheet. They occurred at about 10, 25, 38, 44, and 48 ps. The oscillation of the potential energy for the first two collisions, i.e., from 10 to 38 ps, is shown in Fig. 5(b). It can be seen that the oscillation of potential energy is a superposition of two types of motions; one motion with a large amplitude whereas the other motion has a smaller amplitude. The motions asso-

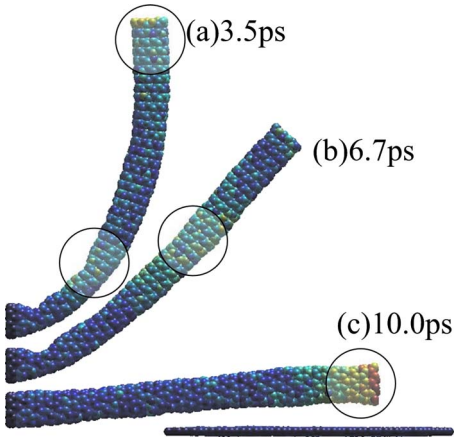

FIG. 3. (Color online) Snapshots on 3.5, 6.7, and 10.0 ps of the CNT in the first scenario (collision of CNT with aspect ratio of 13 and graphene sheet at room temperature) are shown in (a), (b), and (c), respectively. Carbon atoms with high velocity are highlighted and circled and indicating the propagation of kinks.

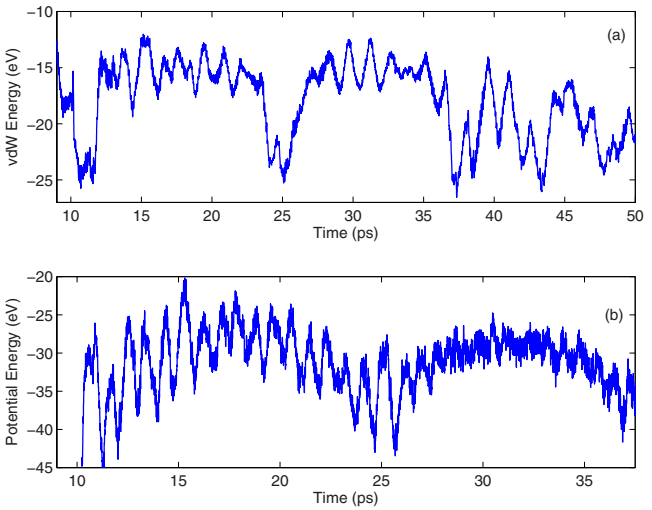

FIG. 5. (Color online) Oscillation of vdW energy and potential energy during collision process in the first scenario (collision of CNT with aspect ratio of 13 and graphene sheet at room temperature).

ciated with the larger amplitude can be attributed to the global movement of carbon atoms, i.e., the deformation of the CNT and graphene sheet. On the other hand, the motions associated with the smaller amplitude can be attributed to the local movement of carbon atoms, i.e., thermal movement. The potential energy can therefore be decomposed into the vdW energy and the internal bond energy where the vdW force is the long-range effect whereas the internal bond force is the short-range effect. The vdW forces play an important role in the deformation of the CNT and graphene sheet while the internal bond energy dominates the thermal movement of carbon atoms. Another observation is that the amplitudes of global motions are decreased after the collision. Therefore, one may deduce that the strain energy has been converted into thermal energy. The average potential energy after the first collision process, i.e., from 15 to 20 ps, can be calculated as −27 eV and this value reduces to −29 eV after the second collision process (i.e., from 30 to 35 ps). From an energy viewpoint, the strain energy is lost due to the collision and the energy loss ratio is about 7.5%. This is significantly different from the elastic macrocollision process between conventional materials, such as glass, steel, and tungsten[30] where the energy loss in an elastic collision is close to zero.

In the second and third scenarios, the strain energy release process and the behaviors of kinks are rather similar to those of the system described in the first scenario, i.e., the propagation of the kinks results in the alternate conversion of potential and kinetic energies. In the second scenario (that investigates the temperature effect), the potential energy of the bent CNT is fully released at 10.0 ps, which is the same as that in the first scenario. However, the speed of the top end atoms of the CNT is 6320 m/s which is higher than 4260 m/s in the first scenario due to the strong thermal motions of carbon atoms under a high temperature. In the third scenario (that investigates the effect of different aspect ratios of CNT), due to the larger bending rigidity of the shorter CNT, the potential energy of the bent CNT is fully released at 6.0 ps, which is faster than 10.0 ps of the longer CNT. Consequently, the speed of the atoms at the top end of the CNT increases to 7570 m/s. The higher speed of the atoms in the second and third scenarios has a significant effect on the impact pressure and will be discussed in detail in Sec. III B.

B. Momentum and impact pressure

In discussing the feasibility of CNTs and graphene functioning as a nanoknife and a nanocutting board, it is instructive to start with the momentum of the graphene sheet. The amount of momentum that graphene sheet possesses can be calculated by taking the product of two physical quantities: the mass and velocity of the carbon atoms. According to Newton's second law, the rate of change in the momentum of the graphene sheet is proportional to the resultant force acting on the graphene sheet. As mentioned above, there are several strong collision processes in the various scenarios but we shall discuss only the first collision processes since the carbon atoms at the boundary are still in a motionless state. Hence, the rate of the change in the momentum of the graphene sheet is totally the impact force at the collision site.

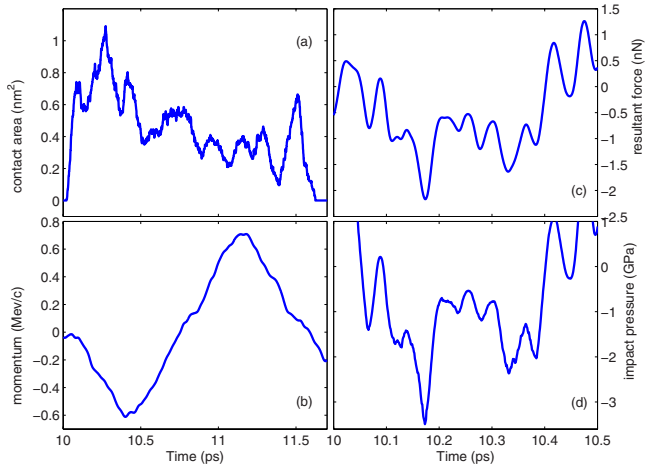

FIG. 6. (Color online) Transit variables, i.e., contact area, momentum, resultant force, and impact pressure, in collision process in the first scenario (collision of CNT with aspect ratio of 13 and graphene sheet at room temperature).

The average impact pressure can therefore be quantified by this resultant force divided by the contact area between CNT and graphene sheet. The definition of contact between atoms is different for that at the macroscale level. Owing to the repulsive vdW effect, the atoms in nanoscale will never touch in the way of contact at the marcroscale. Contact between two atoms is therefore reached when the distance between the two atoms is less than 0.34 nm, which is the equilibrium distance between two graphene layers in graphite. Hence, the contact area can be obtained by multiplying the number of carbon atoms in contact in the graphene sheet with the area of each carbon atom taken as $\sqrt{3}/4 \times (0.142)^2$ nm^2.

Momentum, resultant force, contact area, and impact pressure in graphene sheet are plotted in Fig. 6 for the first scenario. The side view of the deformation of the CNT and graphene sheet is shown in Fig. 7 and the top view of the contact area in the graphene sheet is shown in Fig. 8. In Fig. 6(a), it can be seen that the collision occurs at 10.1 ps and ends at approximately 11.7 ps with a variation in the contact area that indicates an elastic-to-elastic impact. The collision causes a significant deformation in the CNT and graphene

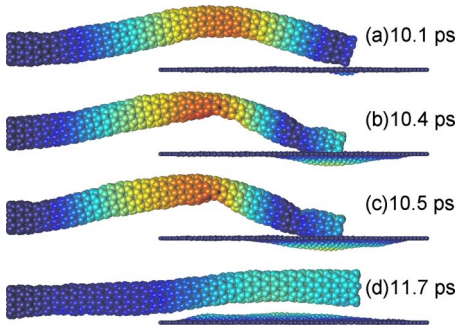

FIG. 7. (Color online) Snapshots of the motions in the first scenario (collision of CNT with aspect ratio of 13 and graphene sheet at room temperature). (a) CNT deforms and touches graphene sheet, (b) CNT tip flattens into a pancake shape due to the contact pressure, (c) maximum deflection of graphene, and (d) CNT rebounds off the graphene sheet. Carbon atoms with high strains concentration at CNT wall are highlighted in at the kinks.

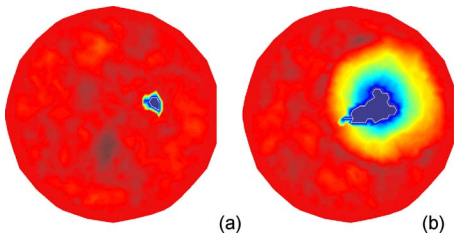

FIG. 8. (Color online) Snapshots of transverse displacement of graphene sheet in the first scenario (collision of CNT with aspect ratio of 13 and graphene sheet at room temperature) and the contact area. (a) 10.1 ps and (b) 10.4 ps.

sheet as shown in Fig. 7. The CNT first deforms and touches the graphene at 10.1 ps. The CNT touches the graphene sheet in a point-to-point contact manner as shown in Fig. 8(a). The downward velocity of carbon atoms due to collision along the transverse direction of graphene sheet results in a negative momentum and resultant force as shown in Figs. 6(b) and 6(c), respectively. The oscillation of the resultant force is probably attributed to the thermal motion of carbon atoms. The negative resultant force and a point type of contact area cause a high impact pressure (of up to approximately 3.6 GPa) as shown in Fig. 6(d). The value of the impact pressure is of the same order as the strength of diamonds,[31] larger than the strength of many known materials. This demonstrates that CNT and graphene sheet can be used as a nanoknife and nanocutting board to cut materials. This impact pressure is so large that the CNT top end flattens into a pancake shape at 10.4 ps as shown in Fig. 7(b). Consequently a point-to-point contact at around 10.1 ps develops into a surface-to-surface contact where the contact area increases to 0.6 nm^2 with an accompanying transverse displacement of 0.23 nm at the center of the graphene sheet as shown in Fig. 8(b). Hence the impact pressure reduces to approximately 2 GPa as shown in Fig. 6(d). At this point, the momentum achieves its maximum magnitude of 0.6 MeV/c, as shown in Fig. 6(c). It indicates the CNT will retract and it starts to retract at 10.5 ps. As a result, the contact area starts to decrease from its maximum value of 1.1 nm^2. The CNT finally rebounds off the graphene sheet at 11.7 ps. At the instant of rebound, the CNT bent into a curved configuration as shown in Fig. 7(d) due to the attractive vdW forces between the CNT and the graphene sheet. The attractive vdW forces also bring about the positive momentum and resultant force. The total contact time of the CNT with the graphene sheet is about 1.6 ps. The CNT and graphene sheet remain completely intact, i.e., they do not fracture or suffer any damage, and they recover fully after the impact. Therefore, the collision between the CNT and graphene sheet can be viewed as an elastic impact even though it is a high speed collision.

The motions of the system in the collision are shown in Fig. 9 for the second scenario and Fig. 10 for the third scenario, respectively. Interestingly the temperature affects the deformation of the CNT and consequently the contact angle (defined as the angle between the axial axis of the CNT with the graphene sheet plane) in the second scenario is smaller than that in the first scenario. The similar reduction in the

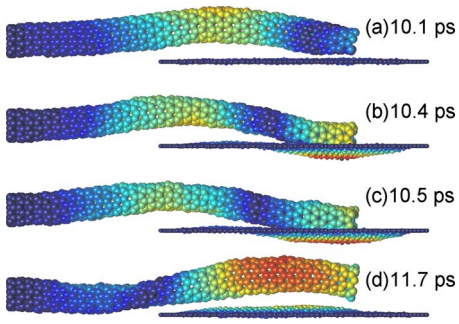

FIG. 9. (Color online) Snapshots of the motions in the second scenario (collision of CNT with aspect ratio 13 and graphene sheet at high temperature, 1500 K). (a) CNT deforms and touches graphene sheet, (b) CNT tip flattens into a pancake shape due to the contact pressure, (c) maximum deflection of graphene, and (d) CNT rebounds off the graphene sheet. Carbon atoms with high strains concentration at CNT wall are highlighted at the kinks.

contact angle also appears in the third scenario due to the effect of aspect ratio of the CNT. With regards to the collision process, the motions of the systems in the second and third scenarios are rather similar to the first scenario. The CNT first deforms and touches the graphene sheet at 10.1 ps and 6.1 ps, respectively. The CNT then retracts, and finally rebounds off the graphene sheet at 11.7 ps and 7.5 ps, respectively. The total contact time of the CNT with the graphene sheet is about 1.4 ps while the CNT and graphene sheet remain completely intact, i.e., they do not fracture or suffer damage. From the energy viewpoint, the strain concentration is higher in the longer CNT as compared with that for the shorter CNT (compare Figs. 7 and 10). Hence a larger proportion of the potential energy in the shorter CNT was transferred to the graphene sheet.

The transit momentum, resultant force, contact area, and impact pressures are shown in Fig. 11 for the second scenario. The system of CNT and graphene sheet appears more "soft" as compared to the first scenario. For example, the maximum contact area increases from 1.1 to 1.8 nm^2 while the accompanying transverse displacement at the center of the graphene sheet maintains at around 0.22 nm, which is similar to 0.23 nm in the first scenario, even though the

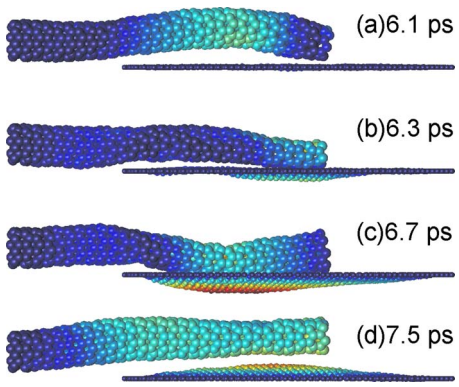

FIG. 10. (Color online) Snapshots of the motions for the third scenario (collision of CNT with aspect ratio of 10 and graphene sheet at room temperature). (a) CNT deforms and touches graphene sheet, (b) CNT tip flattens into a pancake shape due to the contact pressure, (c) maximum deflection of graphene, and (d) CNT rebounds off the graphene sheet. Carbon atoms with high strains concentration at CNT wall are highlighted at the kinks.

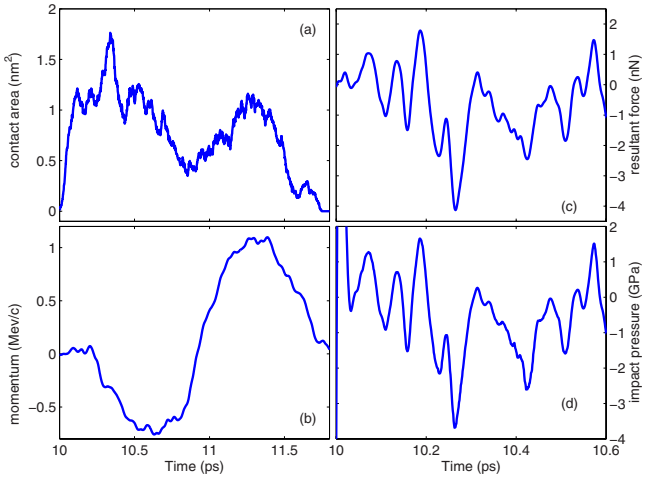

FIG. 11. (Color online) Transit variables, i.e., contact area, momentum, resultant force, and impact pressure, in collision process for the second scenario (collision of CNT with aspect ratio of 13 and graphene sheet at high temperature,1500 K).

speed of top end atoms on the CNT is 6320 m/s as a result of the maximum impact pressure 3.7 GPa, slightly higher than that in the first scenario. The strong oscillation of momentum and resultant force is obviously rooted from the thermal motions of carbon atoms due to the high temperature. The softer phenomenon of CNT and graphene sheet is in line with the observations reported in the literature.[32–34]

The transit momentum, resultant force, contact area, and impact pressures are shown in Fig. 12 for the third scenario. In the third scenario, the collision between CNT and graphene sheet is stronger than that in the first scenario. The maximum contact area is 2.5 nm^2 with an accompanying transverse displacement 0.29 nm, larger than 1.1 nm^2 and 0.23 nm in the first scenario. This indicates that a larger size of material can be cut in the third scenario. The momentum increases to its maximum value of 1 MeV/c from 6.0 to 6.4 ps for the third scenario whereas 0.6 MeV/c from 10.1 to 10.4 ps for the first scenario. The point-to-point contact at an early time results in an extremely high impact pressure up to 10 GPa while this value decreases to 1.8 GPa at 6.2 ps with the increase in contact area. This high impact pressure indicates the cutting process will be easier in the third scenario as compared to the first scenario. Therefore, the aspect ratio of a CNT has a significant effect on the impact pressure. The geometrical dimensions of CNTs and graphene sheet are worth further investigation with the view to optimize the cutting effect utilizing CNTs and graphene sheet as a nanoknife and a nanocutting board.

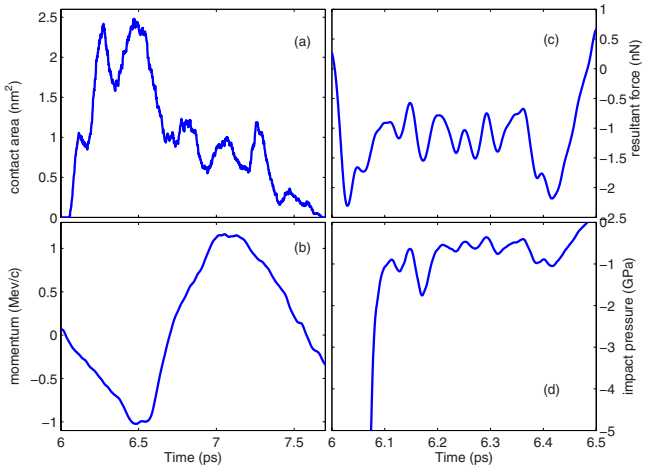

FIG. 12. (Color online) Transit variables, i.e., contact area, momentum, resultant force, and impact pressure, in collision process for the third scenario (collision of CNT with aspect ratio of 10 and graphene sheet at room temperature).

IV. CONCLUSIONS

The present MD simulations show that a CNT has remarkable elastic properties and it is able to store strain energy in kinks in its bent wall. It is worth noting that the velocity of carbon atoms at the tip of a bent CNT can reach 4000 to 7000 m/s by releasing the strain energy. Although the collision between the CNT and graphene sheet is a high speed collision, the CNT and graphene sheet remain completely intact, i.e., they do not fracture or suffer any damage. The maximum deflection of graphene sheet is more than 10% of its radius for the example solved herein. The energy loss ratio during the collision is calculated to be about 7.5% due to the mechanical energy being converted into thermal energy. Interestingly, the impact between CNTs and graphene sheet can result in both positive and negative pressures (attractive force due to the attractive vdW effect). The contact area between the CNT and graphene sheet is estimated to be 1 to 2 nm^2 while the impact pressure is calculated to range from more than 1 to 10 GPa under different temperatures and aspect ratios of CNTs.

The research findings presented herein demonstrate that the CNT and graphene sheet can be used as a nanoknife and cutting board in creating a nanocleavage in materials.

ACKNOWLEDGMENTS

The authors are grateful for the financial support provided by the Australia Research Council (Grant No. ARC DP1095466).

[1] S. Iijima, Nature (London) **354**, 56 (1991).
[2] B. I. Yakobson, M. P. Campbell, C. J. Brabec, and J. Bernholc, Comput. Mater. Sci. **8**, 341 (1997).
[3] E. W. Wong, P. E. Sheehan, and C. M. Lieber, Science **277**, 1971 (1997).
[4] M. F. Yu, O. Lourie, M. J. Dyer, K. Moloni, T. F. Kelly, and R. S. Ruoff, Science **287**, 637 (2000).
[5] M. R. Falvo, G. J. Clary, R. M. Taylor II, V. Chi, F. P. Brooks, Jr., S. Washburn, and R. Superfine, Nature (London) **389**, 582 (1997).
[6] K. M. Liew, X. Q. He, and C. H. Wong, Acta Mater. **52**, 2521 (2004).
[7] K. M. Liew, C. H. Wong, X. Q. He, M. J. Tan, and S. A. Meguid, Phys. Rev. B **69**, 115429 (2004).
[8] K. M. Liew, C. H. Wong, and M. J. Tan, Acta Mater. **54**, 225 (2006).
[9] I. W. Frank, D. M. Tanenbaum, A. M. van der Zande, and P. L. McEuen, J. Vac. Sci. Technol. B **25**, 2558 (2007).
[10] M. Poot and H. S. J. van der Zant, Appl. Phys. Lett. **92**, 063111 (2008).
[11] T. J. Booth, P. Blake, R. R. Nair, D. Jiang, E. W. Hill, U. Bangert, A. Bleloch, M. Gass, K. S. Novoselov, M. I. Katsnelson, and A. K. Geim, Nano Lett. **8**, 2442 (2008).
[12] P. Král and D. Tománek, Phys. Rev. Lett. **82**, 5373 (1999).
[13] T. Chang, Phys. Rev. Lett. **101**, 175501 (2008).
[14] Z. Insepov, D. Wolf, and A. Hassanein, Nano Lett. **6**, 1893 (2006).
[15] Q. Wang, Nano Lett. **9**, 245 (2009).
[16] Q. Wang, Carbon **47**, 1870 (2009).
[17] F. A. Hill, T. F. Havel, and C. Livermore, Nanotechnology **20**, 255704

(2009).
[18]W. Ding, A. Eitan, F. T. Fisher, X. Chen, D. A. Dikin, R. Andrews, L. C. Brinson, L. S. Schadler, and R. S. Ruoff, Nano Lett. **3**, 1593 (2003).
[19]F. J. Rubio-Sierra, W. M. Heckl, and R. W. Stark, Adv. Eng. Mater. **7**, 193 (2005).
[20]H. Xie, D. S. Haliyo, and S. Regnier, Nanotechnology **20**, 215301 (2009).
[21]M. Dienerowitz, M. Mazilu, and K. Dholakia, J. Nanophotonics **2**, 021875 (2008).
[22]J. Liang and J. M. Fernandez, ACS Nano **3**, 1628 (2009).
[23]A. S. Duwez, S. Cuenot, C. Jerome, S. Gabriel, R. Jerome, S. Rapino, and F. Zerbetto, Nat. Nanotechnol. **1**, 122 (2006).
[24]D. Rigby, H. Sun, and B. E. Eichinger, Polym. Int. **44**, 311 (1997).
[25]W. H. Duan, Q. Wang, K. M. Liew, and X. Q. He, Carbon **45**, 1769 (2007).
[26]Q. Wang, W. H. Duan, K. M. Liew, and X. Q. He, Appl. Phys. Lett. **90**, 033110 (2007).
[27]G. X. Cao and X. Chen, J. Mater. Res. **21**, 1048 (2006).
[28]Z. Q. Zhang, H. W. Zhang, Y. G. Zheng, L. Wang, and J. B. Wang, Phys. Rev. B **78**, 035439 (2008).
[29]P. W. Cooper, *Explosives Engineering* (VCH, New York, 1996).
[30]J. Reed, J. Phys. D **18**, 2329 (1985).
[31]D. J. Weidner, Y. B. Wang, and M. T. Vaughan, Science **266**, 419 (1994).
[32]G. Dereli and B. Sungu, Phys. Rev. B **75**, 184104 (2007).
[33]Y. Q. Zhang, X. Liu, and J. H. Zhao, Phys. Lett. A **372**, 1676 (2008).
[34]A. K. Geim, Science **324**, 1530 (2009).